



P-353

## A ray-based offset-to-angle transform for anisotropic medium and its implication in the prestack multicomponent waveform inversion

*Pradip Kumar Mukhopadhyay\* and Subhashis Mallick,*  
*Department of Geology and Geophysics and the School of Energy Resources,*  
*University of Wyoming, Laramie, Wyoming*

### Summary

Offset-to-angle transform is the key element to all reservoir characterization and analysis work. We present a ray-based approach to convert offset domain prestack seismic data into angles. From any given time sample, we ray-trace through the medium to the corresponding source and receiver locations and compute the ray-path length, travel time, offset, and the angle mute for a given angle. We then search for the offset traces that are within the angle mute, locally fit a polynomial to obtain the times corresponding to those offsets and partially stack those offset trace samples to obtain the corresponding zero offset angle domain response. It is straightforward to compute both primary (P-P) and converted wave (P-S) angle gathers using this approach. Although we present our method for a horizontally stratified VTI medium, it can be easily extended to arbitrarily anisotropic dipping layers. Computing theoretical offset domain seismograms for a variety of models and converting them to angles, we verify that we are able to extract accurate response out to large angles. Our new ray-based transform will be useful for AVO/AVA analysis. In addition, it will also be useful for computing accurate angle gathers from observed seismic data and iteratively matching them with synthetic angle gathers in a prestack single or multicomponent waveform inversion for dipping anisotropic medium.

### Introduction

P-P and P-S reflection amplitudes as functions of incidence angle can be calibrated to subsurface lithology and reservoir fluids. Consequently, an accurate offset-to-angle transform is important for all seismic reservoir characterization studies.

Current approach to an offset-to-angle transform is based on the work by Todd and Backus (1985) and Resnick (1993) among others. In this procedure, the angle  $\theta$  for any time sample  $t$  is computed from the relation

$$\sin \theta = \left( \frac{v_{int}}{v_{smooth}} \right) \left\{ \frac{x}{\sqrt{x^2 + (v_{smooth} t_0)^2}} \right\} \quad (1)$$

In equation (1)  $x$  is the source to receiver offset,  $v_{smooth}$  is a spatially varying velocity function derived by smoothing the stacking velocities over a cable length,  $v_{int}$  is the interval

velocity obtained from  $v_{smooth}$ , and  $t_0$  is the two way zero offset travel time. Input prestack seismic data are first compensated for geometrical spreading loss and corrected for normal moveout (NMO). Using equation (1) the source-to-receiver offset  $x$  corresponding to a given angle  $\theta$  for a given time sample is then computed. The seismic trace values for that time sample for the range of offsets lying within the angle mute are then partially stacked to obtain the response for that given angle and for the given time sample. Repeating this operation for all time samples and for all desired values of angles then produces the anglegather. Although such an offset-to-angle transform is for horizontally stratified layers, it can be extended to include dips following the steps given by Resnick et al (1987).

Above procedures for offset-to-angle transform for isotropic layers can be also extended to anisotropic layers by replacing  $v_{smooth}$  with the corresponding anisotropic stacking velocity (Mallick, 2008). It must however be noted



that for anisotropic medium the angle  $\theta$  is the group angle, not the phase angle (for details, see Mallick, 2008).

For P-P reflections, the offset-to-angle transform computed using the above method produces reasonable results for isotropic medium. Its accuracy however, rapidly diminishes with increasing angles for anisotropic medium. For P-S reflections where the NMO equations are complex, such an offset-to-angle transform does not produce reasonable results even for small angles.

Primary purpose of this paper is to present a ray-based offset-to-angle transform that can extract accurate angle domain response for anisotropic medium for both P-P and P-S reflections

### Background Theory

Assume a transversely isotropic medium with a vertical axis of symmetry (VTI medium). In the linearized theory of elasticity, six independent components of the stress tensor are linearly related to the six independent components of the strain tensor as in equation (2)

$$\begin{pmatrix} \tau_{xx} \\ \tau_{yy} \\ \tau_{zz} \\ \tau_{yz} \\ \tau_{zx} \\ \tau_{xy} \end{pmatrix} = \begin{pmatrix} C_{11} & C_{11} - 2C_{66} & C_{13} & 0 & 0 & 0 \\ C_{11} - 2C_{66} & C_{11} & 0 & 0 & 0 & 0 \\ C_{13} & C_{13} & C_{33} & 0 & 0 & 0 \\ 0 & 0 & 0 & C_{44} & 0 & 0 \\ 0 & 0 & 0 & 0 & C_{44} & 0 \\ 0 & 0 & 0 & 0 & 0 & C_{66} \end{pmatrix} \begin{pmatrix} e_{xx} \\ e_{yy} \\ e_{zz} \\ 2e_{yz} \\ 2e_{zx} \\ 2e_{xy} \end{pmatrix} \quad (2)$$

Five independent elastic moduli for a VTI medium are therefore  $C_{11}$ ,  $C_{33}$ ,  $C_{44}$ ,  $C_{66}$ , and  $C_{13}$ . The phase velocity for a VTI medium can be obtained from the solution of the Christoffel equation (Auld, 1973). Consider a plane wave, propagating in the  $x$ - $z$  plane with a given phase angle  $\theta$ . P-wave phase velocity  $V_p(\theta)$  and S-wave phase velocity  $V_{SV}(\theta)$  can then be derived from the solution to the Christoffel equation as (Thomsen, 1986)

$$V_p^2 = \alpha_0^2 [1 + \varepsilon \sin^2 \theta + D^*(\theta)], \quad (3)$$

and

$$V_{SV}^2 = \beta_0^2 [1 + \frac{\alpha_0^2}{\beta_0^2} \varepsilon \sin^2 \theta - \frac{\alpha_0^2}{\beta_0^2} D^*(\theta)], \quad (4)$$

where

$$D^*(\theta) = \frac{1}{2} \zeta \left[ \left\{ 1 + \frac{4\delta^*}{\zeta^2} \sin^2 \theta \cos^2 \theta + \frac{4(\zeta + \varepsilon)\varepsilon}{\zeta^2} \sin^4 \theta \right\}^{\frac{1}{2}} - 1 \right],$$

$$\delta^* = \zeta(2\delta - \varepsilon).$$

$$\zeta = 1 - \frac{\beta_0^2}{\alpha_0^2},$$

$$\varepsilon = \frac{C_{11} - C_{33}}{2C_{33}},$$

$$\delta = \frac{(C_{13} - C_{44})^2 - (C_{33} - C_{44})^2}{2C_{33}(C_{33} - C_{44})},$$

$$\alpha_0 = \sqrt{\frac{C_{33}}{\rho}},$$

and

$$\beta_0 = \sqrt{\frac{C_{44}}{\rho}}.$$

The parameters  $\alpha_0$  and  $\beta_0$  in above are the vertical P- and the S-wave velocities. The inverse of phase velocity is the slowness. Computing slowness for a range of phase angles produces the slowness surface, a section of which in an  $x$ - $z$  plane is pictorially represented in Fig. 1. At any point on this slowness surface, the group velocity vector  $\mathbf{V}_g$  is directed along its normal with magnitude as given in Fig. 1.

Using Fig.1, the group velocity and group angle either for P- or S-wave can be derived as

$$\mathbf{V}_g = [V_{ph}(\theta) \sin \theta + \cos \theta \frac{dV_{ph}}{d\theta}] \hat{\mathbf{x}} + \quad (5)$$

$$[V_{ph}(\theta) \cos \theta - \sin \theta \frac{dV_{ph}}{d\theta}] \hat{\mathbf{z}},$$

$$\tan \phi = \frac{\tan \theta + \frac{1}{V_{ph}} \frac{dV_{ph}}{d\theta}}{1 - \frac{\tan \theta}{V_{ph}} \frac{dV_{ph}}{d\theta}}. \quad (6)$$

In equations (5)-(6),  $\hat{\mathbf{x}}$  and  $\hat{\mathbf{z}}$  are the unit vectors along  $x$  and  $z$  axes respectively and  $V_{ph}(\theta)$  is the phase velocity of either P- or S-wave. While the equations (3) and (4) are for a VTI medium, equations (5) and (6) are valid for a medium with arbitrary anisotropy. Numerically computing the phase velocities for any arbitrarily anisotropic medium



from the Christoffel equation and then computing the group velocities and angles using equations (5) and (6) will therefore allow extending the methodology described here for a general anisotropic medium.

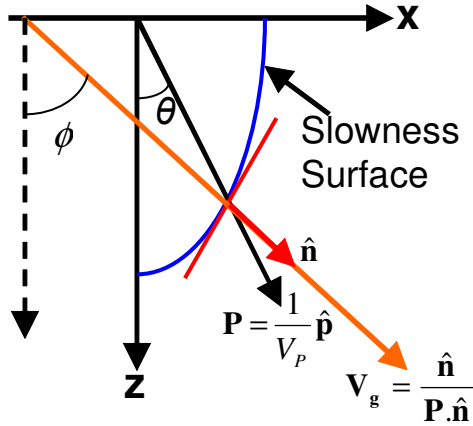


Figure 1: Pictorial representations of phase slowness vector  $\mathbf{P}$ , group velocity vector  $\mathbf{V}_g$ , phase angle  $\theta$ , and group angle  $\phi$  in an anisotropic medium.

### Ray-based offset-to-angle transform

Consider a stack of layers as shown in Fig. 2. The offset  $OA$  for any given group angle  $\theta$  can be calculated by ray tracing the incident ray-path upward through each layer from the given time sample ( $P$ ) to the source and receiver locations ( $A$ ) and by summing the distances from source to reflecting point and from reflecting point to receiver location. For horizontal layers and for surface sources and receivers, the P-P ray-paths from the reflecting point to the source is exactly same as that to the receiver and therefore it is necessary to calculate only one of them. For dipping layers, or for P-SV reflections, or for sources and receivers located at different depths, they are however different, and will require separate computations for each side. Also note that that in an anisotropic medium, while the travel-times and ray-path lengths are calculated from the group velocity and group angle, to refract the rays from one layer to another, it is necessary use equations (3)-(6) to obtain the corresponding phase velocities and angles.

From any time sample and for a given group angle, we therefore calculate the group-velocity immediately above

the sample. We also calculate the ray-parameter corresponding to the given value of the angle. We then calculate the ray-path length, horizontal offset, and travel time for the layer above the sample. As the ray hits an interface with different material properties, we then calculate the corresponding phase velocity and angle, and refract the ray across by preserving the value of the ray-parameter. After refraction, we calculate the group velocity and angle for the new layer and continue this procedure to the source and receiver locations. Summing the travel-time, ray-path length, and horizontal offset from different segments during such ray-tracing gives the total travel-time, ray-path length, and horizontal offset. Note that for dipping layers, the dip angles must also be taken into consideration in addition to the computed ray-parameter to correctly refract rays across each interface. Once these local dips are correctly factored into the ray-parameter, we can apply the same procedure to compute an offset-to-angle transform for a stack of dipping layers.

As we work with NMO uncorrected offset gathers, to partially stack over the angle mutes, we not only need the offsets, but we also need the corresponding times for those offsets. For a given group angle  $\theta$ , we therefore calculate the travel-time, horizontal offset, and ray-path using the above procedure. In addition, we also calculate horizontal offsets and times for a few more angles that are close to  $\theta$  and are within the mute zone. As shown in Fig.2, the ray-paths  $PB$  and  $PC$  are such neighboring ray-paths of  $PA$  with angles that are close to  $\theta$ . As we ray-trace from a given time sample say  $n\Delta t$ , the computed offset values  $OA$ ,  $OB$  and  $OC$  will not necessarily fall on any given offset sample on the input data. This is also true for the calculated travel-times  $BB_1$ ,  $AA_1$ , and  $CC_1$  (see Fig. 2). However, we can use these calculated offsets ( $OA$ ,  $OB$ , and  $OC$ ) and corresponding travel-times ( $BB_1$ ,  $AA_1$ , and  $CC_1$ ) and locally fit a polynomial and use this polynomial to find the times for the corresponding offsets in the data that lie within this mute zone. These time samples can then be stacked and moved to zero-offset time to get the corresponding sample in angle domain. Repeating this procedure for all time samples and for all desired values of angles will give us the angle-gather. Note that our local polynomials are in general different for different angles and therefore correctly handles angle-dependent velocity variations due to anisotropy.



A crucial step in our methodology is the accuracy of the polynomial fitting used to get the exact time samples over the mute zones. We believe that a constrained cubic spline works best for our purpose. In the examples shown here, we used constrained cubic spline interpolation to calculate the travel-times for the range of offsets lying within each mute zone. For best results, the given offset values should be spread uniformly in the mute zone. Alternatively, we can choose the neighboring angle values while ray-tracing in such a way that the calculated offsets fall evenly in the mute zone. This gives an optimum performance of the constrained cubic-spline interpolation. We have also found that using five closely spaced rays gives the most accurate result. Relative merit/demerit of different interpolation methods for offset-to-angle transform in an anisotropic medium will be discussed later in a separate paper.

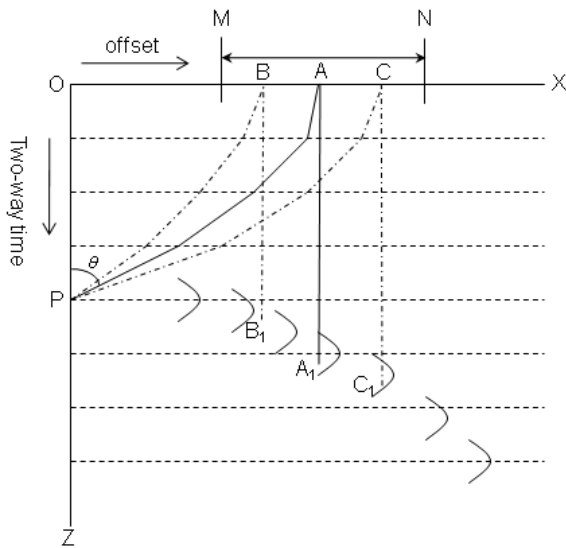
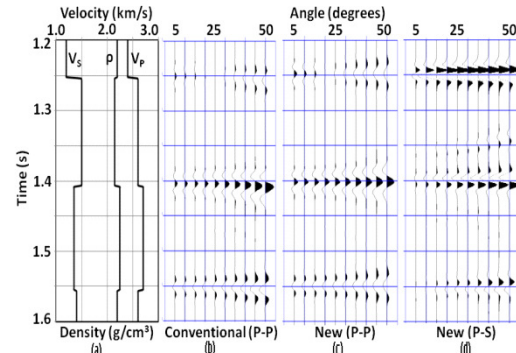


Figure 2: Steps involved in an offset-to-angle transform. For a given two-way zero offset travel time (point P) and a given angle ( $\theta$ ), the corresponding ray-path length (PA), travel time ( $AA_1$ ), offset (OA), and the angle mute (XY) is shown. For neighboring angle values within the mute zone

for which the travel-times and offsets are required for a local polynomial fitting are also shown.

### Synthetic examples

Fig. 3 shows synthetic data computed for a three-layer anisotropic model. Fig. 3(a) is the model. Although the P- and S-wave velocities ( $V_P$  and  $V_S$ ) and density are shown, the model is actually VTI with non-zero values of  $\epsilon$  and  $\delta$ . Fig. 3(b) is the P-P synthetic angle-gather generated from the offset data using a conventional NMO based method and Fig. 3(c) is the corresponding P-P synthetic angle-gather from our new ray-based approach. The P-S synthetic angle-gather from ray-based method is shown in Fig 3(d). Notice that P-S angle gather is shown in two-way P-P time, not in P-S time. One advantage of the ray approach is the fact that it is straightforward to show converted-wave data in P-wave time. This allows a convenient way to jointly



analyze primary and converted-wave data. Also, in order to see the mode-converted events clearly in Fig. 3(d), their amplitudes are magnified by a factor of 10 compared to the corresponding P-P gathers.

Figure 3: (a) Three-layer model (b) P-P angle-gather using conventional method (c) P-P angle-gather using new method (d) P-S angle gathers using new method. P-S amplitudes are magnified by a factor of 10 compared to the P-P amplitudes.

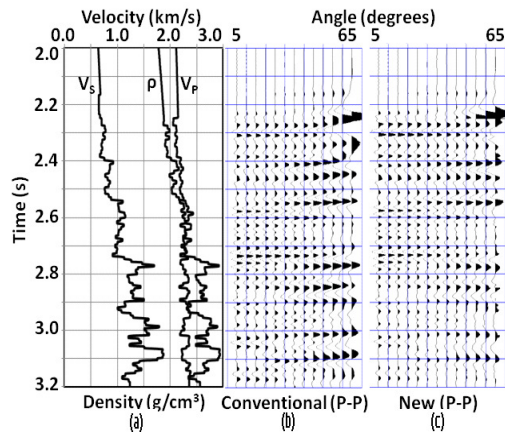


Figure 4: (a) Multilayer earth model (b) P-P angle-gather using conventional method (c) P-P angle-gather using new method.

Fig. 4 shows synthetic data computed for a multilayer anisotropic model. Fig. 4(a) is the model. Similar to Fig. 3(a), only the isotropic parts of the model is shown. Fig. 4(b) is the P-P angle-gather from conventional method and Fig. 4(c) is the angle-gather from the ray-based approach.

## Discussion

Examples shown in Figures 3 and 4 clearly demonstrate the superiority of the ray-based offset-to-angle transformation compared to a conventional approach. Notice that the P-P events in the three-layer example from the conventional method are bent downwards with increasing angles, and for the multilayer case they are bent upwards (Figures 3b and 4b). While such bending of events are controlled the choice of the VTI parameters  $\epsilon$  and  $\delta$ , the reason for this bending is the increasing inaccuracy of the NMO equation for large offsets. By computing the exact travel-times through ray-tracing, we are able to drastically improve the quality of the computed angle gathers. NMO equations for the mode-converted reflections are complex even for an isotropic medium. By accurately computing the mode-converted travel-times, not only we have computed accurate angle gathers but we have also shown a convenient way of displaying them in P-wave times (Figure 3d) so that they can be jointly compared with P-P reflections in an AVO/AVA analysis. Waveform based inversions are now

rapidly emerging as valuable tools for predicting subsurface lithology and fluid properties. Our ray-based offset-to-angle transforms could be directly incorporated into such inversions. As discussed, it is straightforward to account for dips and any arbitrary anisotropy into our transform methodology. Starting with an initial model of dipping anisotropic layers, we can iteratively compute angle domain responses using our method and match with corresponding full-waveform synthetic angle-gathers to invert observed seismic data for a stack of dipping anisotropic layers. Convenience of obtaining both primary and mode-converted data in two-way P-P travel-times allows investigating the possibility of using such a method for both single (P-wave) and multicomponent waveform inversions.

## Conclusions

Computing an accurate angle-gather is crucial to predicting subsurface lithology and fluid properties from seismic data. While a conventional NMO based offset-to-angle transform is increasingly inaccurate with increasing angles, ray-based method allows accurate calculation of angle-gathers at large angles. Computing accurate converted wave angle-gathers in P-wave times allows a convenient way for joint analysis of primary and mode-converted reflection responses in AVO/AVA. Although we demonstrate our methodology for horizontally stratified VTI medium, it can be easily extended to arbitrarily anisotropic dipping layers. Finally, it is straightforward to incorporate our technique into a waveform inversion scheme to invert observed single- or multicomponent seismic data for a stack of dipping anisotropic layers.

## References

- Auld B. A., 1973, *Acoustic Fields and Waves: 1*, J. Wiley, New York
- Bansal, R., and Sen, M.K, 2007, Inversion of fracture parameters in laterally varying media using ray-Born approximation: 77<sup>th</sup> Ann. Internat. Mtg., Soc. Expl. Geophys., Expanded Abstracts, 1898-1902.
- Ferguson, R.J., and Sen. M.K, 2002,  $\tau$ -p domain estimation of elastic parameters in VTI media: 72<sup>nd</sup> Ann. Internat. Mtg., Soc. Expl. Geophys., Expanded Abstracts, 169-172.



## A ray-based offset-to-angle transform for anisotropic medium



Mallick, S., 1999, Some practical aspects of prestack waveform inversion using a genetic algorithm: an example from the east Texas Woodbine gas sand: *Geophysics*, **64**, 326-336.

Mallick, S., 2000, Waveform inversion of multicomponent seismic data: 70<sup>th</sup> Ann. Internat. Mtg., Soc. Expl. Geophys., Expanded Abstracts, 2273-2276.

Mallick, S., 2001, AVO and elastic impedance: The Leading Edge, 1094-1104.

Mallick, S., 2007, Amplitude-variation-with-offset, elastic-impedence, and wave-equation synthesis – A modeling study: *Geophysics*, **72**, C1-C7.

Mallick, S., 2008, Interpretation of angle gathers for transversely isotropic medium: 78<sup>th</sup> Ann. Internat. Mtg., Soc. Expl. Geophys., Expanded Abstracts, 2937-2941.

Ostrander, W. J., 1984, Plane-wave reflection coefficients for gas sands at nonnormal angles of incidence: *Geophysics*, **49**, 1637-1648.

Resnick, J.R., 1993, Seismic data processing for AVO and AVA analysis, in J.P. Castagna and M.M. Backus, eds., 1993, *Offset-Dependent Reflectivity- Theory and Practice for AVO Analysis*: Soc. Expl. Geophys., 175-189.

Resnick, J.R., Ng, P., and Larner, K., 1987, Amplitude versus offset analysis in the presence of dip: 57<sup>th</sup> Ann. Internat. Mtg., Soc. Expl. Geophys., Expanded Abstracts, 617-620.

Sen, M.K., and Mukherji, A., 2000, Reflection moveout analysis and waveform inversion in transversely isotropic media: 70<sup>th</sup> Ann. Internat. Mtg., Soc. Expl. Geophys., Expanded Abstracts, 2249-2252.

Sen, M.K., and Stoffa, P.L., 1992, Genetic inversion of AVO: *The Leading Edge*, **11**, 27-29.

Smith, G.C., and Gidlow, P. M., 1987, Weighted stacking for rock property estimation and detection of gas: *Geophysical Prospecting*, **35**, 993-1014.

Stolt, R.H., and Weglein, A.B., 1985, Migration and inversion of seismic data: *Geophysics*, **50**, 2458-2472.

Thomsen, L., 1986, Weak elastic anisotropy: *Geophysics*, **51**, 1954-1966.

Thomsen, L., 1999, Converted-wave reflection seismology over inhomogeneous, anisotropic media: *Geophysics*, **64**, 678-690.

Todd, C.P., and Backus, M.M., 1985, Offset-dependent reflectivity in a structural context: 55<sup>th</sup> Ann. Internat. Mtg., Soc. Expl. Geophys., Expanded Abstracts, 586-588.

### Acknowledgments

This research is funded by the US Department of Energy Grant DE-NT0004730.